Journal of Power Sources 197 (2012) 97–101

Contents lists available at SciVerse ScienceDirect

Journal of Power Sources

journal homepage: www.elsevier.com/locate/jpowsour

Short communication

Electrodeposition of PVA-protected PtCo electrocatalysts for the oxygen reduction reaction in H_2SO_4

Luiz H.S. Gasparotto*, Eduardo G. Ciapina, Edson A. Ticianelli, Germano Tremiliosi-Filho

Instituto de Química de São Carlos, Universidade de São Paulo, 13560-970 São Carlos, SP, Brazil

ARTICLE INFO

Article history:
Received 5 July 2011
Received in revised form 6 September 2011
Accepted 9 September 2011
Available online 16 September 2011

Keywords:
PtCo electrodeposition
PVA
Oxygen reduction reaction

ABSTRACT

In this paper we report the electrosynthesis of PVA-protected PtCo films (PVA = poly(vinylalcohol)) and their activities towards the oxygen reduction reaction (ORR). PtCo electrodeposits were potentiostatically obtained in the presence and absence of PVA at distinct potentials. The film morphology and composition were characterized by scanning electron microscopy (SEM) and energy-dispersive X-ray spectroscopy (EDX), which revealed that the use of PVA in the electrodeposition of PtCo films was decisive to achieve better film composition control. Cyclic voltammetry for PVA-protected PtCo films showed that the electrochemical surface area is dependent on the electrodeposition potentials and suggested different adsorption strengths of oxygen-containing species. Films produced in the presence of PVA presented the following activity order towards ORR as a function of the electrodeposition potential (*vs.* Ag/AgCl): −0.9 V > −0.8 V > −1.0 V > −0.7 V. In contrast, PtCo films electrodeposited in the absence of PVA displayed very similar activities regardless of the electrodeposition potential. The simplicity of the electrodeposition method combined with its effectiveness enabled the production of "model electrodes" for investigating the fundamental aspects of the reactions taking place in the fuel cell cathodes.

1. Introduction

Fuel cells have attracted a global attention in recent decades due to their high theoretical efficiency and environmental compatibility [1]. However, some technical and economical issues, such as the poor kinetics of the cathodic reaction (oxygen reduction reaction: ORR), excessive catalyst loading and costs, must be overcome in order to make commercially viable fuel cells. One way to enhance the cathodic performance is to alloy Pt with other metals such Co, Ni and Fe, since they have presented good potential alternative as Pt-modified catalysts for ORR kinetics [2–4]. Among different Pt alloys, PtCo has been extensively studied since it has higher electrocatalytic activity towards ORR compared to other Pt-based alloys [5,6].

Recently, Woo et al. [7] galvanostatically produced PtCo catalysts on carbon for proton exchange membrane fuel cells (PEMFC). They found that the electrochemical method of production improved the control of the catalyst layer thickness and enhanced the performance of the tested cells. Saejeng and Tantavichet [1] prepared PtCo catalysts through pulse current electrodeposition onto pretreated electrodes. The electrochemical mode and the pulse plating parameters did not significantly affect the PtCo composition. On the other hand, the variation of Pt concentration in the electrolytic bath led to profound changes in the Pt/Co ratio. The best composition, for the studied parameters, was Pt:Co 82:18. In addition, the performance can be further increased by employing the electrocatalyst in the nanometric regime [8]. Electrodeposition has proved to be a very effective method for nanomaterial fabrication since it is rapid and facile, allowing easy control of the nucleation and growth through electrode potential manipulation. The avoidance of a chemical reducing agent enhances the purity of the particles. Allied with the use of protective agents (e.g. poly(vinylalcohol) (PVA) [9] and poly(vinylpyrrolidone) (PVP) [10]), electrochemistry has been extensively and successfully employed in the controlled fabrication of nanostructured materials [10–14]. Although PVA is commonly employed as capping agent, its influence on the stability of the PtCo alloy in acid solutions and on the electrochemical activity towards the oxygen reduction reaction is completely unknown.

The aim of this work was to investigate the ORR in acid solution at potentiostatically prepared PVA-protected PtCo catalysts. The film morphology and composition were characterized by scanning electron microscopy (SEM) and energy-dispersive X-ray spectroscopy (EDX), while cyclic voltammetry was used to evaluate the electrocatalytic activity toward O_2 reduction. The influences of PVA on the film composition and morphology as well as on the ORR are discussed.

* Corresponding author. Tel.: +55 16 3373 9934; fax: +55 16 3373 9903.
E-mail address: lhgasparotto@iqsc.usp.br (L.H.S. Gasparotto).

0378-7753/$ – see front matter © 2011 Elsevier B.V. All rights reserved.
doi:10.1016/j.jpowsour.2011.09.019

2. Experimental

H_2PtCl_6, $CoCl_2$ and PVA (MW: ~50.000; 80% hydrolyzed) were purchased from Aldrich Co. and used without further purification. The solution for PtCo film electrodeposition consisted of 3 mmol L^{-1} H_2PtCl_6 + 0.11 mol L^{-1} $CoCl_2$ + 1% (w/w) PVA + 0.1 mol L^{-1} KCl. Prior the electrodepositions, a gold rotating-disk electrode (*Area* = 0.28 cm^2) embedded in PTFE was polished with 1500 grid carbide paper, followed by 9 μm and 3 μm alumina. The electrode was then sonicated for 10 min in ultrapure Milipore/Milli-Q water in order to remove alumina residues, followed by 10 voltammetric cycles in the potential range 0.05 V–1.8 V *vs.* reversible hydrogen electrode (RHE) in O_2-free 0.5 mol L^{-1} H_2SO_4 to remove, if any, remaining impurities. All potentials are referred to the RHE unless otherwise stated. Films with different compositions were deposited onto the clean gold rotating-disk electrode at distinct potentials of −0.7 V, −0.8 V, −0.9 V and −1.0 V *vs.* Ag/AgCl. A platinum sheet served as counter electrode. After the electrodepositions the rotating disk electrode was thoroughly rinsed with ultrapure water, inserted into a conventional three-electrode cell and subjected to 10 voltammetric cycles between 0.05 and 1.0 V *vs.* RHE at a scan rate of 50 mV s^{-1} followed by 3 cycles at 20 mV s^{-1} to remove impurities remaining from the electrodeposition bath. The electrochemical Pt surface areas of the electrodes were calculated via the H_{upd} desorption charge, considering a conversion factor of 210 μC cm^{-2} for polycrystalline Pt [15,16]. Rotating disk electrode experiments for the oxygen reduction were conducted in an O_2-saturated 0.5 mol L^{-1} H_2SO_4 at room temperature (~25 °C). Potentiodynamic sweeps were carried out at 1600 rpm with a scan rate of 5 mV s^{-1}.

All electrochemical measurements were carried out using an AUTOLAB 30 potentiostat/galvanostat controlled by the GPES software. Scanning electron microscopy (SEM) and energy-dispersive X-ray spectroscopy (EDX) were conducted on a Zeiss-Leica/440 to determine the morphology and composition of the films. For the SEM and EDX analyses, PtCo films were electrodeposited onto gold sheets (10 mm × 10 mm × 1 mm) in a Teflon cell clamped over a Teflon covered Viton o-ring under the same above-mentioned electrodeposition conditions.

3. Results and discussion

3.1. PtCo electrodeposition

Fig. 1 presents cyclic voltammograms (CV) for the gold electrode at 50 mV s^{-1} in 3 mmol L^{-1} H_2PtCl_6 + 0.11 mol L^{-1} $CoCl_2$ + 0.1 mol L^{-1} KCl in the absence (black line) and presence of 1% PVA (red line). A CV for the gold electrode in O_2-free 0.1 mol L^{-1} KCl (supporting electrolyte) is also presented for comparison. Starting the sweep at 0.5 V *vs.* Ag/AgCl towards negative potentials, the cathodic currents between 0.07 V and −0.33 V *vs.* Ag/AgCl are higher than those in the supporting electrolyte. These currents are due to platinum electrodeposition [17]. As the scan progressed, multiple cathodic waves were observed between −0.33 V and −0.7 V *vs.* Ag/AgCl in either absence or presence of PVA. Yasin et al. [18] showed that, although the voltammograms for carbon and gold in H_2PtCl_6 displayed multiple cathodic waves, they all result from the reduction of Pt(IV) to Pt(0) and there is no evidence for Pt(II) as a stable intermediate at any potential. The multiple waves appear as a consequence of the hexachloroplatinic acid speciation, since it exists in solution as a mixture of kinetically inert Cl^-/H_2O complexes [18]. The reduction processes between −0.33 V and −0.7 V *vs.* Ag/AgCl in the presence of PVA are shifted towards more positive potentials. This is probably a consequence of the chelating properties of the PVA [19], which, due to its interaction with the different Pt species, led to distinct reduction potentials.

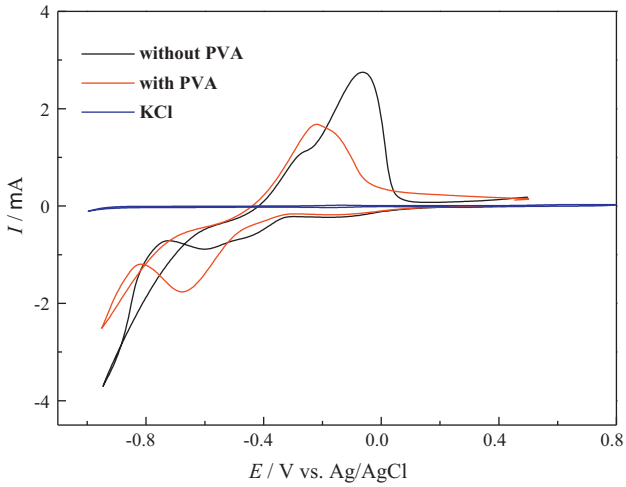

Fig. 1. Cyclic voltammograms for gold at a scan rate of 50 mV s^{-1} in 3 mmol L^{-1} H_2PtCl_6 + 0.11 mol L^{-1} $CoCl_2$ + 0.1 mol L^{-1} KCl with and without 1% (w/w) PVA.

Cobalt electrodeposition sets in at potentials negative to −0.7 V *vs.* Ag/AgCl in the PVA-free solution (black line) and −0.8 V *vs.* Ag/AgCl in the PVA-containing solution (red line), clearly demonstrating that PVA affects the Co deposition. This is also evidenced by the lower magnitude of the cathodic currents observed in the PVA-containing solution in this potential range. Later we will show that the presence of PVA is of pivotal importance for controlling the composition of the film. During the back scan the CV exhibited a current crossover (typical for a nucleation-controlled process) and the anodic currents between −0.4 V and 0 V *vs.* Ag/AgCl are related to Co dissolution. The distinct anodic potential peaks suggest that PtCo alloys were formed with different Pt/Co ratios. (For interpretation of the references to color in this paragraph, the reader is referred to the web version of the article.)

3.2. SEM characterization

Fig. 2 shows a series of SEM images of PtCo films obtained on the gold substrate in the PVA-containing solution at distinct potentials of −0.7 V, −0.8 V, −0.9 V and −1.0 V *vs.* Ag/AgCl maintained for 1 min. At −0.7 V *vs.* Ag/AgCl (Fig. 2A) the substrate is poorly covered with very small nanoparticles hardly recognizable at this magnification. The substrate scratches caused by polishing are still clearly visible and the EDX analysis revealed the deposited particles to be Pt. Holding the potential at −0.8 V *vs.* Ag/AgCl (Fig. 2B) the aspect of the substrate changes distinctly as Co was also electrodeposited (revealed by EDX). A thin electrodeposit layer covers the substrate whose scratches are now less recognizable. Decreasing the potential to −0.9 V *vs.* Ag/AgCl (Fig. 2C) the Co deposition becomes more intense and the characteristic film morphology is evident. Similar deposit morphologies have been observed for pure PtCo on titanium [20] and pure Co on glassy carbon [21], which further supports the Co film enrichment. At −1.0 V *vs.* Ag/AgCl (Fig. 2D) the particle size drastically decreases and the deposit layer takes over the substrate. Table 1 presents the potential-dependent film composition determined by EDX, confirming higher amounts of Co with potential decrease. For comparison, PtCo compositions for films electrodeposited in the absence of PVA are also displayed in Table 1. It is clear that a poor film composition control is achieved in the absence of PVA.

3.3. Cyclic voltammetry for PtCo in 0.5 mol L^{-1} H_2SO_4

Cyclic voltammograms (CVs) recorded at 50 mV s^{-1} in O_2-free 0.5 mol L^{-1} H_2SO_4 for all PtCo films obtained in the PVA-containing

Table 1
Atomic compositions, electroactive area, oxide reduction peak potentials and half-wave potentials of all PtCo films employed in this work.

Electrodeposition potential/V *vs.* Ag/AgCl (3 M)	EDX atomic nominal composition		Electrochemical active Pt surface area/cm^2		Oxide reduction peak potential/V		$E_{1/2}$/V (RHE) for the ORR 1600 rpm, 5 mV s^{-1}	
	With 1% PVA	Without PVA	With 1% PVA	Without PVA	With 1% PVA	Without PVA	With 1% PVA	Without PVA
−0.7 V	Pt (100%)	$Pt_{20}Co_{80}$	0.43	1.10	N/A[a]	0.809	0.773	0.835
−0.8 V	$Pt_{70}Co_{30}$	$Pt_{10}Co_{90}$	1.30	1.43	0.786	0.814	0.849	0.838
−0.9 V	$Pt_{25}Co_{75}$	Pt_5Co_{95}	2.65	1.16	0.806	0.810	0.889	0.841
−1 V	$Pt_{10}Co_{90}$	Pt_4Co_{96}	1.14	1.12	N/A[a]	0.813	0.838	0.835

[a] For the electrodeposits formed at −0.7 and −1.0 V, the position of the oxide reduction peak could not be determined with confidence.

and PVA-free solutions at distinct potentials are shown in Fig. 3. The PtCo films prepared in the PVA-containing solution (Fig. 3A) exhibited an ill-defined current profile in the Pt H_{upd} region (0.05–0.4 V *vs.* RHE), despite the large proportion of Pt in the deposits. The CV currents are higher for the PVA-protected electrodeposits, particularly for that obtained at −0.9 V *vs.* Ag/AgCl. This means that the surface blocking by PVA may be not so pronounced. In this sense the CV may represent just the behavior of a true PtCo surface. Oxidation/reduction currents above 0.7 V *vs.* RHE are characteristic of the formation of oxygen-containing species, however processes related to adsorbed PVA oxidation cannot be discarded. The distinct electrodeposition potentials delivered different electrochemical active surface areas. Electrodeposits prepared at −0.9 V *vs.* Ag/AgCl exhibited the highest currents in the hydrogen adsorption/desorption region, followed by those formed at −1.0 V and −0.8 V (both presented similar currents) and −0.7 V *vs.* Ag/AgCl. In Table 1 the calculated electrochemical active surface areas are shown for all electrodes, which confirms the qualitative trend described above. In contrast, all electrodeposits prepared in the absence of PVA (Fig. 3B) exhibited similar current magnitudes as a result of comparable electrochemical surface areas (Table 1). Moreover, the CVs depicted a more defined Pt H_{udp} region when compared to those films obtained in the presence of PVA, characteristic of Pt rich surfaces in acid media [22,23]. Platinum bimetallic alloys with 3d transition metals such as Ni, Co, Fe, among others, are known to be unstable materials in respect to the surface dissolution of the less noble element in acid electrolytes [24–27], forming a structure with a Pt-rich layer generally known as "Pt-skeleton" [26,27]. The similarities of the cyclic voltammograms in Fig. 3B indicate that the effect of Co dissolution is more drastic for the electrodeposits produced in the PVA-free solution. An important observation was that, just after immersion of the films produced in the PVA-free solution into the acid electrolyte, formation of small bubbles on the film surface was readily visible and the open circuit potential (OCP) was 0 V *vs.* RHE. Thermodynamic data [28] show that the $Co \rightarrow Co^{2+} + 2e^-$ with the simultaneous formation of molecular hydrogen by the reaction $2H^+ + 2e^- \rightarrow H_2$ is a spontaneous chemical redox reaction. The formation of H_2 bubbles, therefore, explains the OCP of 0 V *vs.* RHE as a consequence of the H^+/H_2 equilibrium. In contrast, all electrodeposits obtained in the PVA-containing solution neither exhibited the same qualitatively effect observable by naked eye nor the behavior of the OCP. This result suggests that PVA helped in preventing Co dissolution.

An important finding observed in the CVs of Fig. 3 is related to the position of the oxide reduction peaks (negative-going sweep) for the PtCo films (see Table 1). According to several works [26,27,29], differences in the position of the oxide reduction peaks can be

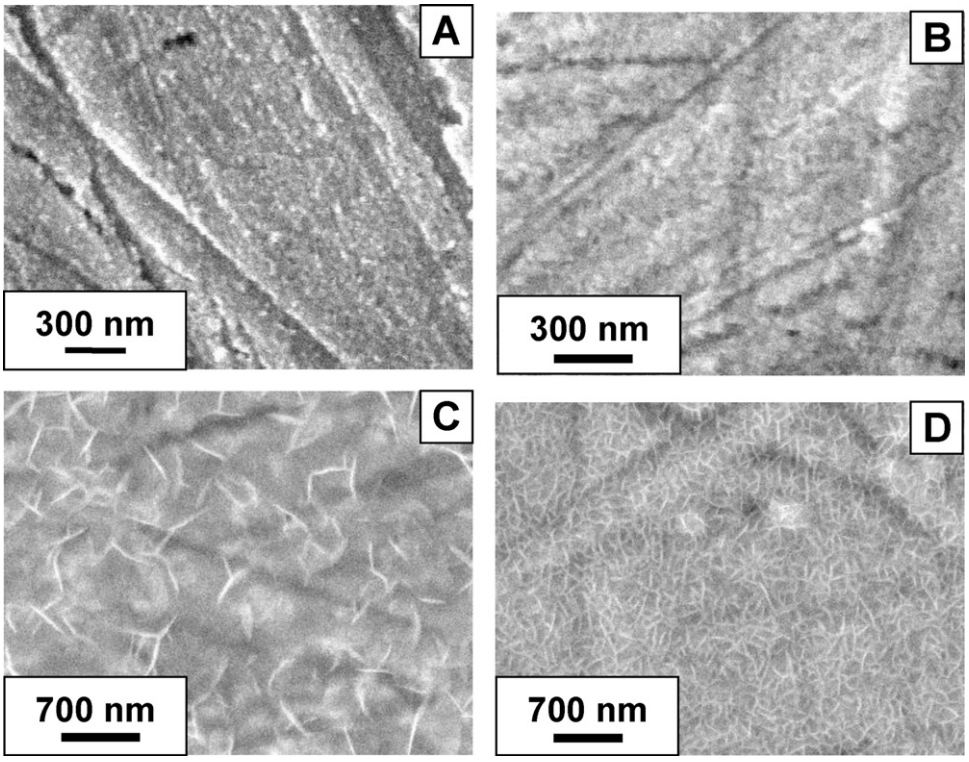

Fig. 2. SEM images of PtCo obtained in 1% (w/w) PVA + 3 mmol L^{-1} H_2PtCl_6 + 0.11 mol L^{-1} $CoCl_2$ + 0.1 mol L^{-1} KCl at (A) −0.7 V, (B) −0.8 V, (C) −0.9 V and (D) −1.0 V *vs.* Ag/AgCl.

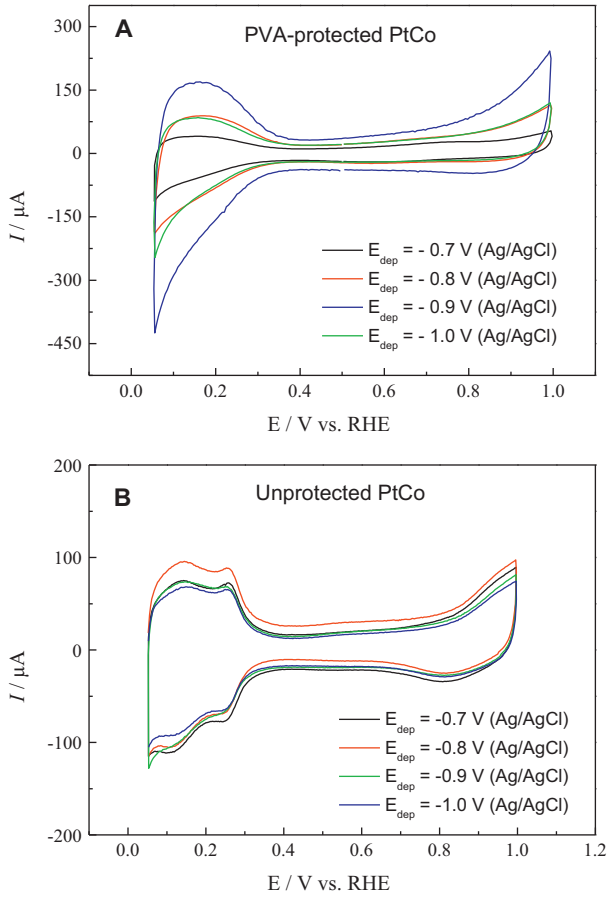

Fig. 3. Cyclic voltammograms for PtCo films electrodeposited at distinct potentials in (A) PVA-containing and (B) a PVA-free solutions. Data recorded at a scan rate of 50 mV s^{-1} in an O_2-free 0.5 mol L^{-1} H_2SO_4 solution.

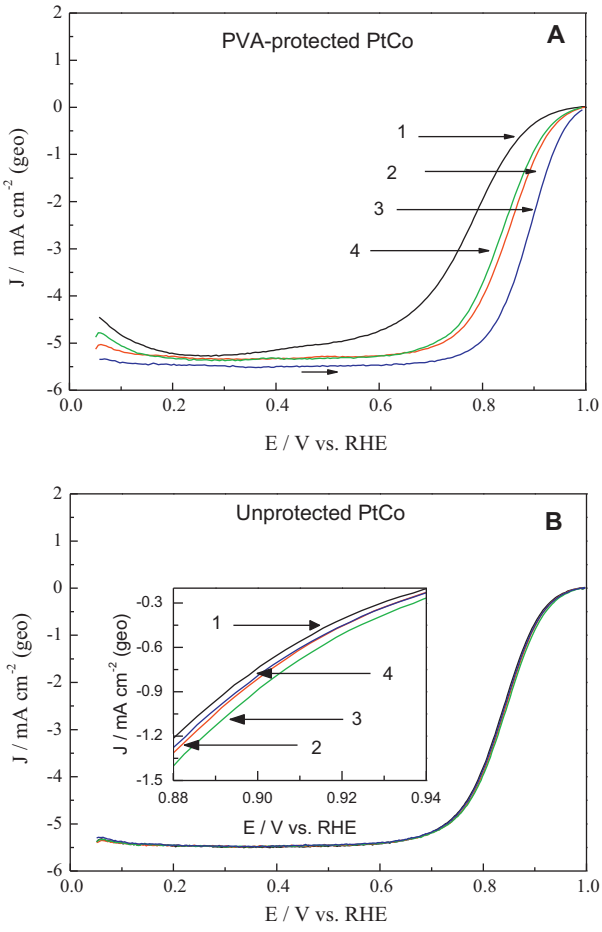

Fig. 4. Rotating disk electrode experiments for the oxygen reduction reaction on PtCo films electrodeposited at distinct potentials (1) −0.7 V, (2) −0.8 V, (3) −0.9 V and (4) −1.0 V *vs.* Ag/AgCl in (A) PVA-containing solution and (B) PVA-free solution. Data are shown for the positive-going sweep at 5 mV s^{-1} and 1600 rpm in O_2-saturated 0.5 mol L^{-1} H_2SO_4 solution. Currents densities normalized by the geometric area.

assigned to different adsorption strengths of oxygen-containing species. In general, the higher the reduction overpotential, the stronger is the interaction. This effect is usually explained by downshifts in the d-band center caused by subsurface 3d alloying elements [30,31]. Assuming that this consideration is valid, one concludes that the film obtained at −0.8 V *vs.* Ag/AgCl in the PVA-containing solution presents a stronger interaction with oxygenated species when compared to the films electrodeposited at −0.9 V *vs.* Ag/AgCl in the same conditions, since there is a small but significant difference of 20 mV towards less positive potentials in the peak positions. Among the electrodeposits obtained in the PVA-free solution there are only minor differences in the oxide reduction peak (8 mV or less), indicating more similar adsorption strengths of oxygenated species. These features are of paramount importance in the electrocatalysis of the oxygen reduction reaction, as discussed in the following section.

3.4. Oxygen reduction reaction (ORR)

Rotating disk electrode (RDE) experiments were carried out (Fig. 4) in O_2-saturated 0.5 mol L^{-1} H_2SO_4 at 5 mV s^{-1} and 1600 rpm to obtain ORR kinetics for the PtCo electrodeposits produced in the presence and absence of PVA. In general, the diffusion limited current density for all electrodeposits were about 5.5 mA cm^{-2}, which is in agreement with published data obtained under similar experimental conditions [32–34]. Fig. 4A shows these results for the PVA-protected PtCo electrodeposited at distinct potentials (i.e. −0.7 V, −0.8 V, −0.9 V and −1.0 V *vs.* Ag/AgCl). The values of half-wave potentials ($E_{1/2}$, listed in Table 1) clearly indicate that the PtCo films produced in the PVA-containing solution at distinct potentials have different activities. A huge difference of 116 mV was found between the $E_{1/2}$ of the PVA-protected PtCo films electrodeposited at −0.7 V and −0.9 V *vs.* Ag/AgCl, with the later displaying the highest electrochemical activity. In terms of electrodeposition potential, the activities at the $E_{1/2}$ potential followed the order (*vs.* Ag/AgCl): −0.9 V > −0.8 V > −1.0 V > −0.7 V. Correlating with the EDX data, the best initial film composition for ORR corresponded to $Pt_{25}Co_{75}$. In contrast, as seen in Fig. 4B, all the PtCo films electrodeposited in the absence of PVA displayed very similar activities, showing only minor current variations (inset in Fig. 4B) and negligible differences in the half-wave potentials (Table 1). As previously reported, hydrogen is readily formed upon the PVA-unprotected PtCo film exposition to the acid medium. Consequently, Co leaches to the solution and the surfaces of the films are then constituted of pure Pt (confirmed by EDX), explaining the coincidental activities. This result further supports the hypothesis that PVA prevented drastic Co dissolution.

Although the $E_{1/2}$ may give a quantitative measure of the activity of the distinct electrodes, its value is influenced by the active electrochemical surface area. Note that the current densities shown in Fig. 4 were reported in terms of the geometric area of the electrode and, therefore, do not reflect the specific activities (the current per active surface area, in units of μA cm^{-2}_{real}) of the distinct PtCo films. In order to compare the specific activity among the several electrodeposits, the currents must be correct for mass-transport

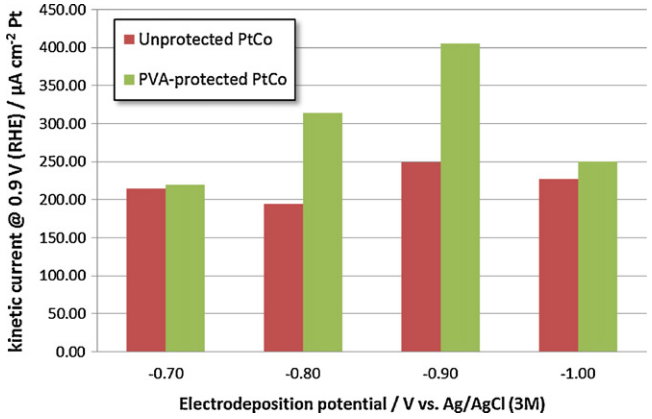

Fig. 5. Kinetic current densities (specific activities) obtained at 0.9 V (RHE) for PtCo films produced in PVA-containing and PVA-free solutions at different electrodeposition potentials.

process according to the following equation [35], and then normalized by the active surface area:

$$i_k = (i_d \times i)/(i_d - i)$$

where "i" is the measured current, "i_d" is the diffusion-limited current and "i_k" is the kinetic current. Specific activities at 0.9 V *vs.* RHE calculated from the RDE experiments for all electrodeposits are shown in Fig. 5. The specific activities of the electrodeposits prepared in the presence of PVA exhibited a strong dependence with the electrodeposition potential. This variation can be correlated with the distinct initial nominal atomic composition (Table 1). As suggested by Markovic et al. [29], the composition modulates the Pt 5d-band center and, therefore, the adsorptive properties of Pt-based catalysts, leading to different strengths of interaction between Pt and oxygen-containing species. Since the ORR is a multi-step reaction involving adsorbed intermediates [30,36], it is expected that changes in the adsorption properties affect the catalytic activity towards the ORR. The CVs for PtCo films electrodeposited at −0.8 V and −0.9 V *vs.* Ag/AgCl (Fig. 3A) in the PVA-containing solution did show significant increase of the potential of the oxide reduction peak in the negative-going sweep (see Table 1). Inspection of Fig. 5 reveals ORR specific activities of 313.7 and 405.8 μA cm^{-2} for the PtCo films produced at −0.8 V and −0.9 V *vs.* Ag/AgCl, respectively. The clear superior electrocatalytic activity presented by the former can be correlated to an increase of 20 mV in the oxide reduction peaks (from 0.79 V to 0.81 V *vs.* RHE) of the just-mentioned PtCo films (see Table 1). On the other hand, the PtCo films produced in the PVA-free solution presented similar values for the oxide reduction peak (about 0.81 V *vs.* RHE), and therefore the specific activities exhibited minor variations.

In spite of the good correlation between the oxide reduction peaks and the electrochemical activities, a possible influence of PVA cannot be ruled out. The oxide reduction potential peak of the PtCo films electrodeposited at −0.9 V *vs.* Ag/AgCl presented very similar values (0.81 V) regardless of electrodeposition media (with or without PVA), but the electrochemical activity was higher for films obtained in the presence of PVA (Fig. 5). Although the presence of PVA at the catalyst surface may influence the ORR, to date, however, the literature completely lacks about the role of PVA in the electrocatalysis of ORR. Further surface analysis (FTIR) will be carried out in the future in order to clarify this point.

4. Conclusions

The use of PVA in the electrodeposition of PtCo films was decisive to achieve better film composition control and high activities for ORR. The ORR activities for films produced in PVA-containing solutions were directly dependent on the electrodeposition potentials, while films electrodeposited in the PVA-free solutions displayed roughly coincidental ones regardless of the applied potential. Electrodeposition has proved to be a valuable tool for the production of nanostructured catalysts, which can be regarded as "model electrodes" for investigating the fundamental aspects of the reactions taking place in fuel cells.

Acknowledgements

The authors thank FAPESP, CNPq and CAPES for the financial support.

References

[1] Y. Saejeng, N. Tantavichet, J. Appl. Electrochem. 39 (2009) 123–134.
[2] S. Mukerjee, S. Srinivasan, M.P. Soriaga, J. McBreen, J. Electrochem. Soc. 142 (1995) 1409–1422.
[3] S. Mukerjee, S. Srinivasan, J. Electroanal. Chem. 357 (1993) 201–224.
[4] Q.G. He, S. Mukerjee, Electrochim. Acta 55 (2010) 1709–1719.
[5] A.K. Shukla, M. Neergat, P. Bera, V. Jayaram, M.S. Hegde, J. Electroanal. Chem. 504 (2001) 111–119.
[6] L. Xiong, A.M. Kannan, A. Manthiram, Electrochem. Commun. 4 (2002) 898–903.
[7] S. Woo, I. Kim, J.K. Lee, S. Bong, J. Lee, H. Kim, Electrochim. Acta 56 (2011) 3036–3041.
[8] E. Roduner, Chem. Soc. Rev. 35 (2006) 583–592.
[9] Z.H. Mbhele, M.G. Salemane, C. van Sittert, J.M. Nedeljkovic, V. Djokovic, A.S. Luyt, Chem. Mater. 15 (2003) 5019–5024.
[10] B.S. Yin, H.Y. Ma, S.Y. Wang, S.H. Chen, J. Phys. Chem. B 107 (2003) 8898–8904.
[11] Yu, S.-S. Chang, C.-L. Lee, C.R.C. Wang, J. Phys. Chem. B 101 (1997) 6661–6664.
[12] X. Hong, G. Wang, W. Zhu, X. Shen, Y. Wang, J. Phys. Chem. C 113 (2009) 14172.
[13] W. Pan, X.K. Zhang, H.Y. Ma, J.T. Zhang, J. Phys. Chem. C 112 (2008) 2456–2461.
[14] H.Y. Ma, B.S. Yin, S.Y. Wang, Y.L. Jiao, W. Pan, S.X. Huang, S.H. Chen, F.J. Meng, Chemphyschem 5 (2004) 68–75.
[15] S. Trasatti, O.A. Petrii, J. Electroanal. Chem. 327 (1992) 353–376.
[16] F.C. Nart, W. Vielstich, Handbook of Fuel Cells: Fundamentals Technology and Applications, John Wiley & Sons, Chichester, 2003.
[17] J.J. Mallett, E.B. Svedberg, S. Sayan, A.J. Shapiro, L. Wielunski, T.E. Madey, P.J. Chen, W.F. Egelhoff Jr., T.P. Moffat, Electrochem. Solid-State Lett. 8 (2005) C15–C18.
[18] H.M. Yasin, G. Denuault, D. Pletcher, J. Electroanal. Chem. 633 (2009) 327–332.
[19] S. Clemenson, L. David, E. Espuche, J. Polym. Sci. Part A: Polym. Chem. 45 (2007) 2657–2672.
[20] C. Xu, Y. Su, L. Tan, Z. Liu, J. Zhang, S. Chen, S.P. Jiang, Electrochim. Acta 54 (2009) 6322–6326.
[21] Q.-S. Chen, S.-G. Sun, J.-W. Yan, J.-T. Li, Z.-Y. Zhou, Langmuir 22 (2006) 10575–10583.
[22] J. Solla-Gullon, P. Rodriguez, E. Herrero, A. Aldaz, J.M. Feliu, Phys. Chem. Chem. Phys. 10 (2008) 1359–1373.
[23] E.G. Ciapina, S.F. Santos, E.R. Gonzalez, J. Electroanal. Chem. 644 (2010) 132–143.
[24] S. Chen, W. Sheng, N. Yabuuchi, P.J. Ferreira, L.F. Allard, Y. Shao-Horn, J. Phys. Chem. C 113 (2009) 1109–1125.
[25] J. Greeley, J.K. Nørskov, Electrochim. Acta 52 (2007) 5829–5836.
[26] V.R. Stamenkovic, N.M. Markovic, Handbook of Fuel Cells: Fundamentals, Technology and Applications, John Wiley & Sons, New York, 2003.
[27] V.R. Stamenkovic, B.S. Mun, K.J.J. Mayrhofer, P.N. Ross, N.M. Markovic, J. Am. Chem. Soc. 128 (2006) 8813–8819.
[28] C.M.A. Brett, A.M.O. Brett, Electrochemistry: Principles, Methods and Applications, Oxford University Press, New York, 1993.
[29] C. Wang, M. Chi, G. Wang, D. van der Vliet, D. Li, K. More, H.-H. Wang, J.A. Schlueter, N.M. Markovic, V.R. Stamenkovic, Adv. Funct. Mater. 21 (2011) 147–152.
[30] J.R. Kitchin, J.K. Norskov, M.A. Barteau, J.G. Chen, J. Chem. Phys. 120 (2004) 10240–10246.
[31] J. Greeley, I.E.L. Stephens, A.S. Bondarenko, T.P. Johansson, H.A. Hansen, T.F. Jaramillo, J. Rossmeisl, I. Chorkendorff, J.K. Norskov, Nat. Chem. 1 (2009) 552–556.
[32] T. Ghosh, M.B. Vukmirovic, F.J. DiSalvo, R.R. Adzic, J. Am. Chem. Soc. 132 (2009) 906.
[33] U.A. Paulus, A. Wokaun, G.G. Scherer, T.J. Schmidt, V. Stamenkovic, N.M. Markovic, P.N. Ross, Electrochim. Acta 47 (2002) 3787–3798.
[34] U.A. Paulus, A. Wokaun, G.G. Scherer, T.J. Schmidt, V. Stamenkovic, V. Radmilovic, N.M. Markovic, P.N. Ross, J. Phys. Chem. B 106 (2002) 4181–4191.
[35] E. Gileadi, Electrode Kinetics. For Chemists, Chemical Engineers, and Materials Scientists, VCH, New York, 1993.
[36] J.K. Nørskov, J. Rossmeisl, A. Logadottir, L. Lindqvist, J.R. Kitchin, T. Bligaard, H. Jónsson, J. Phys. Chem. B 108 (2004) 17886–17892.